Lamb wave devices using capacitive micromachined ultrasonic transducers

G. G. Yaralioglu,[a] M. H. Badi, A. S. Ergun, C. H. Cheng, and B. T. Khuri-Yakub
Ginzton Laboratory, Stanford University, Stanford, California 94305

F. L. Degertekin
George W. Woodruff School of Mechanical Engineering, Georgia Institute of Technology, Atlanta, Georgia 30332

Lamb wave devices based on capacitive micromachined ultrasonic transducers (CMUTs) have been built on 500-μm-thick silicon wafers for frequencies in the vicinity of 1 MHz. CMUTs have been used to both excite and detect Lamb waves in the substrate. This configuration eliminates the need for piezoelectric materials, which are not compatible with the existing integrated circuit (IC) fabrication techniques, and allows easy integration of Lamb wave devices and electronics on the same wafer. Finite element analysis of the devices shows that the lowest order antisymmetric Lamb wave (A_0) is the dominant mode in the substrate in this frequency range. This result is also confirmed by demonstration experiments. © *2001 American Institute of Physics.*
[DOI: 10.1063/1.1337647]

Lamb wave and surface acoustic wave (SAW) devices are being used in many applications from simple transversal filters to gas detectors.[1,2] Traditional Lamb wave and SAW devices use piezoelectricity to generate ultrasonic waves in the substrate on which they are built. Electrodes are arranged in interdigital configuration on piezoelectric substrates or with piezoelectric films such as lead zirconium titanate, lithium niobate, zinc oxide, and others.[3–6] However, these materials are not compatible with the existing integrated circuit fabrication processes. This limits the integration of Lamb wave or SAW devices with the electronics. Instead of piezoelectricity, using capacitive micromachined ultrasonic transducers (CMUTs) for generation and detection of acoustic waves in the substrate has greater potential for electronic integration. This results in inexpensive integrated circuits for mass production and devices with increased noise performance, because the cabling between the transducers and the electronics is eliminated.

The CMUT has been used to generate and detect ultrasonic waves only for liquid immersion and air-borne applications so far.[7–9] A CMUT consists of a metalized silicon nitride membrane supported by posts and it is built on a silicon wafer using standard micromachining techniques. The electrode on the membrane and the highly doped silicon substrate form a parallel plate capacitor, which is used to generate and detect ultrasonic waves in the immersion medium. When a voltage is applied between the metalized membrane and the substrate, electrostatic forces attract the membrane toward the substrate. Stress within the membrane and the bending stiffness of the membrane resist the attraction. Driving the membrane with a time harmonic signal one generates acoustic waves in the immersion medium. Since the electrostatic forces are always attractive, for a sinusoidal motion, a bias voltage should be added to the ac drive. CMUTs can also be used for the detection of ultrasound. A

biased membrane under impinging acoustic field can generate significant currents.

The CMUT membranes are generally considered clamped at their edges and most of the previous work has focused on the interaction of the membrane and the ultrasonic waves in the immersion medium. However, recent experiments have shown that these devices couple energy not only into the medium they are immersed in but also to the substrate they are built on. Radiation pattern measurements in liquid media clearly identified the leaky Lamb wave propagation in the substrate due to vibrating CMUT membranes.[10] The coupling between the membranes and the silicon substrate occurs through the membrane supports. In this letter, we report devices that are optimized for coupling energy into the particular Lamb wave propagation mode of the substrate.

One element of the Lamb wave transducer is shown in Fig. 1. Many of these membranes are used together to form a Lamb wave transducer. We followed the same fabrication steps that are used for circular CMUTs.[9] The dimensions of the membrane are 100 μm and 1 cm as indicated in Fig. 1. The thickness of the membrane and the air gap are both 1 μm. The metal electrode covers half of the membrane area and its thickness is negligibly small compared to the thick-
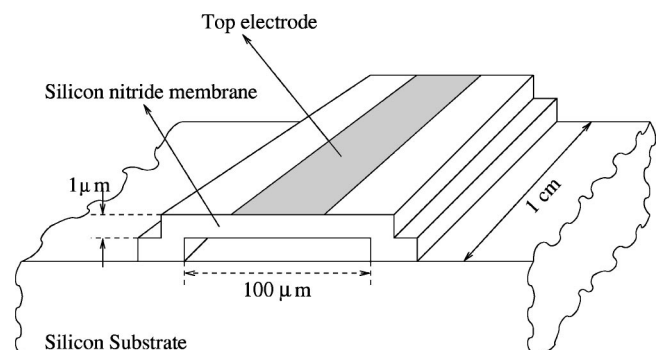

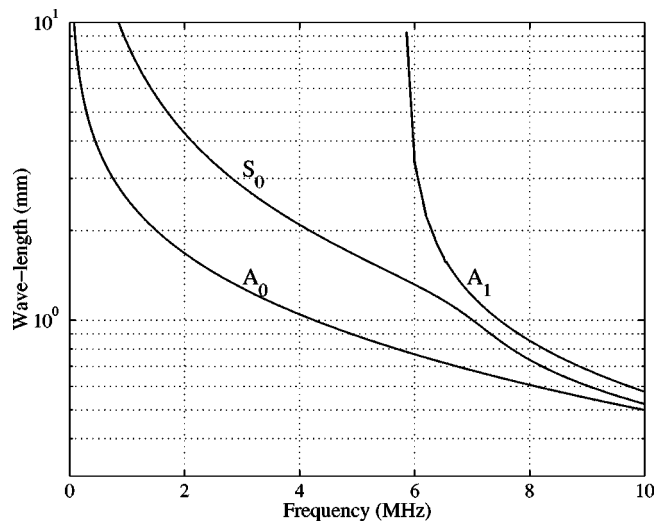FIG. 1. Schematic of a single rectangular CMUT. The membrane gap is 1 μm.

FIG. 2. Lamb wave dispersion curves in the $\langle 110 \rangle$ orientation. For silicon we used the following elastic coefficients; $c_{11} = 165.7$ GPa, $c_{12} = 63.9$ GPa, $c_{44} = 79.56$ GPa and rotated them 45° around the Z axis.

FIG. 3. Calculated propagated power generated by a single membrane. Membrane is assumed to be in vacuum. Silicon nitride membrane is 100 μm wide and 1 μm thick. The air gap is also 1 μm. The tension in the membrane is assumed to be 100 MPa. The silicon substrate is $\langle 110 \rangle$ oriented and the thickness is 500 μm.

ness of the membrane. The substrate is a highly doped 500-μm-thick (100) silicon wafer. The rectangular CMUT is perpendicular to the $\langle 110 \rangle$ crystal orientation. This crystal axis is chosen to be in the direction of the Lamb wave propagation since it has the minimum diffraction loss.[11]

We performed finite element (FE) calculations[12] and normal mode decomposition[11,13] to identify the propagating modes in the substrate for the single membrane shown in Fig. 1. It is crucial to find the distribution of power among different modes to be able to design an optimum device. We used FE analysis to determine the distribution of particle displacement and stress components along the thickness of the substrate resulting from the sinusoidal membrane vibration. We performed two-dimensional calculations since the length of the membrane is substantially larger than its width. To avoid the reflections of the propagating waves from the edges of the substrate, we employed absorbing boundaries at the silicon ends by means of a lossy medium of considerable length.[14,15] We calculated the field distribution close to the edge of the absorbing region and employed normal mode decomposition. For a 500 μm silicon wafer, the lowest order symmetric S_0 and antisymmetric A_0 Lamb waves are the only propagating modes below 5 MHz as shown in Fig. 2. The total propagating power as well as the power radiated by the A_0 and S_0 modes are depicted in Fig. 3. The radiated power is maximum at the resonance frequency. It is evident that most of the total power (more than 90%) is carried by A_0 at low frequencies, whereas as the frequency increases S_0 becomes more significant. The quality factor of the resonance curves in Fig. 3 is relatively large ($>10\,000$). In these FE calculations, we assumed that the membrane is in vacuum. Moreover, we included the residual stresses by stretching the membrane from the sides. For our fabrication variables, the residual stress in the silicon nitride membranes is typically 100 MPa.

Since the CMUT membrane couples more power to the A_0 mode, the spacing between the fingers of an A_0 mode Lamb wave device should be designed according to the wavelength of this mode. The Lamb wave device consisting of several CMUT membranes in parallel is shown in Fig 4.
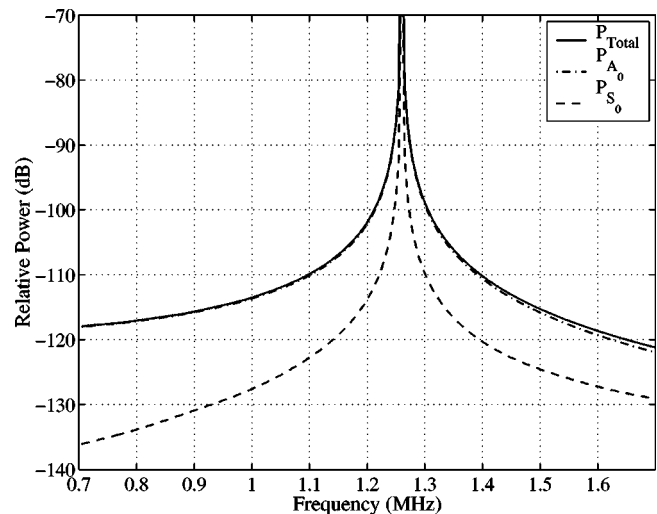
The membrane resonance frequency and the acoustic wavelength in the substrate determine the device geometry. The resonance frequency of the membrane of Fig 1 is 1.26 MHz. At this frequency, the A_0 mode wavelength is 2.5 mm in the $\langle 110 \rangle$ direction of the 500-μm-thick silicon plate (Fig. 2). For optimum A_0 excitation, the width and the periodicity of the fingers should be $\lambda/4$ and λ, respectively.[16] Hence, each finger contains five, 100-μm-wide, 1-cm-long membranes.

To test the devices, we used the setup shown in Fig 4. First, we measured the impedance of a finger which is composed of five membranes. Figure 5 depicts the measurement result. Note that this measurement has been taken in air. We found that the resonance frequency is at 1.5 MHz, which is
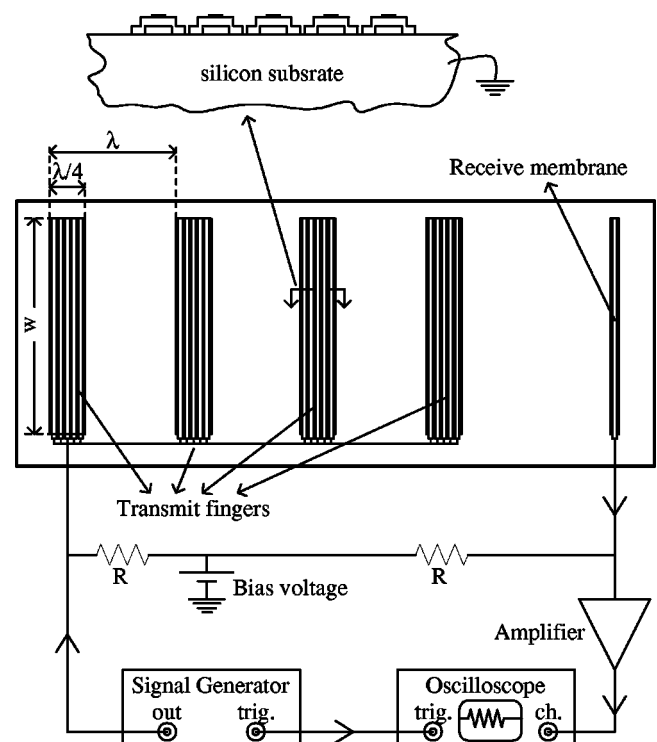

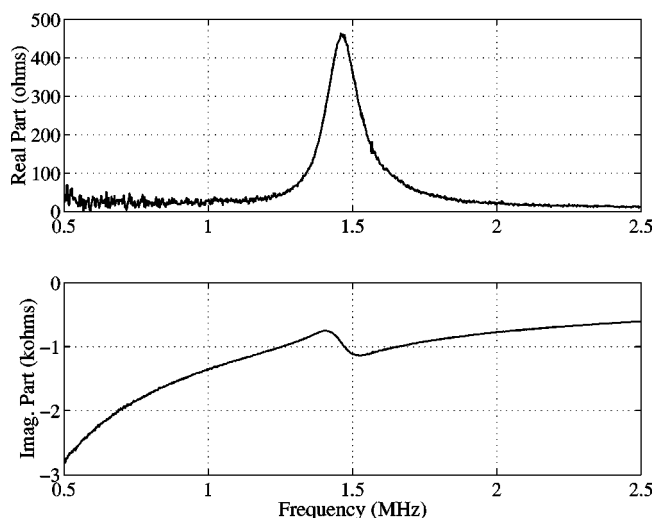FIG. 4. The Lamb wave device and test setup.

FIG. 5. Measured impedance of a finger in air. Bias voltage is 70 V. Note that each finger has five membranes in parallel.

FIG. 6. Transmission measurement in air.

slightly higher than the calculated resonance frequency 1.26 MHz shown in Fig. 3. This mismatch can be attributed to the squeezed film effect. Our first generation devices are not sealed, hence there is an air cushion in the membrane gap. This air cushion increases the stiffness of the membrane, resulting in higher resonance frequency. In vacuum, the resonance frequency of the membranes is measured to be 1.25 MHz.

For transmission measurements, we used another device with transmit and receive membranes separated by a large distance to obtain clean signals. The distance between the receiver and the transmitter is approximately 3.87 mm. This device operates at 1.8 MHz in air. A rf-tone burst of one cycle at 1.8 MHz from the function generator is applied to the transmit fingers. The output from the receive membrane is monitored by the oscilloscope after 60 dB amplification as depicted in Fig. 4. Figure 6 shows both the calculated and measured received signals. In the calculations, we assumed line sources at the membrane locations and to find the source function we simply convolved the membrane transfer function with the electrical signal on the electrode. We modeled the membrane motion by the simple harmonic oscillator. We calculated the temporal Fourier transform of the source field and propagated each frequency component with the phase velocity determined by the calculated A_0 mode dispersion relation. Finally, inverse Fourier transform and convolution with the membrane transfer function gives the electrical output at the receive membrane. Our calculations predict the arrival time of the measured signal quite well. The phase difference between the calculated and the measured data in Fig. 6 is due to the electrical parasitic capacitances which are not included in the calculations.

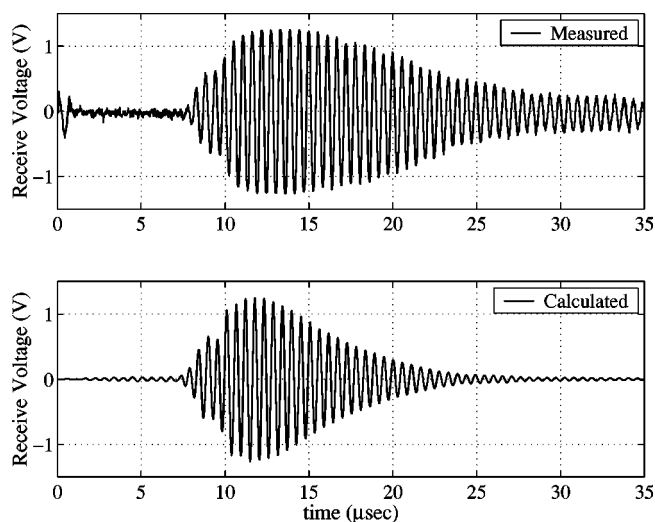In summary, we showed the feasibility of Lamb wave generation and detection in silicon by CMUTs, eliminating the need for piezoelectricity. We used silicon micromaching techniques for device fabrication. We have verified our FE and analytical calculations by experiments on devices operating in the 1 MHz frequency range. Based on these results, we plan to change the fabrication steps for improved coupling and to fabricate high frequency SAW devices in the 100 MHz frequency range.

[1] G. S. Kino, *Acoustic Waves: Devices, Imaging, and Analog Signal Processing* (Prentice-Hall, Englewood Cliffs, NJ, 1987).
[2] C. K. Campbell, *Surface Acoustic Wave Devices for Mobile and Wireless Communications* (Academic, San Diego, CA, 1998).
[3] D. F. Fischer, W. J. Varhue, J. Wu, and C. A. Whiting, J. Microelectromech. Syst. **9**, 88 (2000).
[4] E. Moulin, J. Assaad, and C. Delebarre, J. Appl. Phys. **82**, 2049 (1997).
[5] S. W. Wenzel and R. M. White, IEEE Trans. Electron Devices **35**, 735 (1988).
[6] M. J. Vellekoop, G. W. Lubking, P. M. Sarro, and A. Venema, Sens. Actuators A **44**, 249 (1994).
[7] M. I. Haller and B. T. Khuri-Yakub, IEEE Ultrasonics Symposium Proceedings, Cannes, France, November 1994, p. 1241.
[8] H. T. Soh, I. Ladabaum, A. Atalar, C. F. Quate, and B. T. Khuri-Yakub, Appl. Phys. Lett. **69**, 3674 (1996).
[9] I. Ladabaum, X. Jin, H. T. Soh, A. Atalar, and B. T. Khuri-Yakub, IEEE Trans. Ultrason. Ferroelectr. Freq. Control **45**, 678 (1998).
[10] X. C. Jin, F. L. Degertekin, S. Calmes, X. J. Zhang, I. Ladabaum, and B. T. Khuri-Yakub, IEEE Ultrasonics Symposium Proceedings, Sendai, Japan, October 1998, p. 1877.
[11] B. A. Auld, *Acoustic Fields and Waves in Solids* (Wiley, Toronto, 1973), Vol. 2.
[12] For the FEA calculations we used ANSYS5.6.
[13] F. L. Degertekin and B. T. Khuri-Yakub, Appl. Phys. Lett. **69**, 146 (1996).
[14] A. Bozkurt, F. L Degertekin, A. Atalar, and B. T. Khuri-Yakub, IEEE Ultrasonics Symposium Proceedings, Sendai, Japan, October 1998, p. 1025.
[15] E. Moulin, J. Assaad, C. Delebarre, and D. Osmont, J. Acoust. Soc. Am. **107**, 87 (2000).
[16] I. A. Viktorov, *Rayleigh and Lamb Waves: Physical Theory and Applications* (Plenum, New York, 1967).